ITP-94-30E
July 1994

Deuteron Electromagnetic Form Factors in the Transitional Region Between Nucleon-Meson and Quark-Gluon Pictures

A. P. Kobushkin and A. I. Syamtomov

N.N.Bogolyubov Institute for Theoretical Physics,
National Academy of Sciences of Ukraine, Kiev 143, Ukraine

Abstract

Experimental observables of the elastic eD-scattering in the region of intermediate energies are discussed. We offer the analysis of the available experimental data, which reproduces the results of the calculations with popular NN-potentials at low energies ($Q^2 \ll 1(GeV/c)^2$), but, at the same time, provides the right asymptotic behavior of the deuteron e.m. form factors, following from the quark counting rules, at high energies ($Q^2 \gg 1(GeV/c)^2$). The numerical analysis developed allows to make certain estimations of the characteristic energy scale, at what the consideration of quark-gluon degrees of freedom in the deuteron becomes essential.

1 Introduction

It was already demonstrated [1-3], that the quark substructure of the deuteron should manifest itself in the elastic *ed*-scattering at high Q^2. Nevertheless, up to now the question of the energy scale at what quark-gluon degrees of freedom become defrozen in simplest nuclear systems has been remaining a subject of great interest (see e.g. Ref. [4]). It seems that the so called quark counting rules [5] applied to the elastic *ed*-scattering at high Q^2 give the most natural way for estimating of such scale. While QCD predicts [6, 7] that the individual asymptotic behavior of deuteron form factors will differ significantly from that predicted by the conventional NN-potential models, the predicted asymptotic behavior of the cross section $\frac{d\sigma}{dt} \sim \frac{1}{t^{11}} f(t/s)$ (where s and t are the conventional Mandelstam variables) can be also reproduced within the "classical" (nucleon-meson) picture [8]. Therefore, it is a topical matter to look for another observables of the elastic *ed*-scattering which could be sensitive to the quark-gluon structure of the deuteron.

The aim of the present paper is to study the behavior of the elastic *ed*-scattering in intermediate region between nucleon-meson and quark-gluon pictures and to estimate a Q^2-scale, where QCD consideration becomes valid. We show that the QCD asymptotics sets in the helicity-flip transition amplitudes at Q^2 of order of few $(GeV/c)^2$. The outline of the paper is as follows. In Sec.2 we summarize the general expressions for observables of the elastic *ed*-scattering as well as expressions of the deuteron e.m. form factors in terms of helicity transition amplitudes in the infinite momentum frame. The QCD predictions for the helicity transition amplitudes at high Q^2 are discussed in Sec.3. In Sec.4 we analyze the experimental data for the elastic *ed*-scattering ($A(Q^2)$ and $B(Q^2)$ structure functions, the tensor analyzing power T_{20}), using phenomenological parametrization, which reproduces the results of the nucleon-meson calculations at $Q^2 \ll 1(GeV/c)^2$ and reduces to the asymptotic behavior predicted by the perturbative QCD at $Q^2 \gg 1(GeV/c)^2$. It is assumed that the region where Q^2 are of the order of few $(GeV/c)^2$ is the region where the nucleon-meson calculations as well as pure QCD methods are not applicable. Predictions for the e.m. form factors of the deuteron and T_{20} at Q^2 of the order of few $(GeV/c)^2$ are done. Conclusions are given in Sec.5.

2 Basic relations

In the lab. frame the cross section of the elastic *ed*-scattering (when the particles are unpolarized) is given by the Rosenbluth formula

$$\frac{d\sigma}{d\Omega} = \left(\frac{d\sigma}{d\Omega}\right)_{Mott} \left[A\left(Q^2\right) + B\left(Q^2\right) \tan^2\left(\frac{\theta}{2}\right)\right], \tag{2.1}$$

where $\left(\frac{d\sigma}{d\Omega}\right)_{Mott}$ is the Mott cross section, θ is the electron scattering angle; $A\left(Q^2\right)$ and $B\left(Q^2\right)$ – are the deuteron structure functions, which, in turn, are expressed via the charge, G_C, magnetic, G_M, and qudrupole, G_Q, deuteron form factors:

$$A = G_C^2 + \frac{2}{3}\eta G_M^2 + \frac{8}{9}\eta^2 G_Q^2, \quad B = \frac{4}{3}\eta(1+\eta)G_M^2, \tag{2.2}$$

where $\eta = Q^2/4M^2$ and M is the deuteron mass. To separate the charge and qudrupole form factors one has, in addition to A and B structure functions, to measure polarization observables of the process, e.g. the tensor analyzing power

$$T_{20}(Q^2,\theta) = -\frac{\frac{8}{9}\eta^2 G_Q^2 + \frac{8}{3}\eta G_C G_Q + \frac{2}{3}\eta G_M^2\left[\frac{1}{2} + (1+\eta)\tan^2\left(\frac{\theta}{2}\right)\right]}{\sqrt{2}\left[A\left(Q^2\right) + B\left(Q^2\right)\tan^2\left(\frac{\theta}{2}\right)\right]}. \tag{2.3}$$

The normalization of the form factors entering (2.2) and (2.3) is chosen to be the following: $G_C(0) = 1,\ G_M(0) = \frac{2M}{e}\mu_D$, $G_Q(0) = \frac{M^2}{e}Q_D$, where μ_D and Q_D are the deuteron magnetic and qudrupole moments, respectively. In the infinite momentum frame, defined as in Ref. [9], the form factors could be expressed in terms of the helicity transition amplitudes [10] $J^{\mu}_{\lambda'\lambda} =< p'\ \lambda'|j^{\mu}|p\ \lambda >$:

$$\begin{aligned}
G_C &= \frac{1}{2p^+(2\eta+1)}\left[(1-\frac{2}{3}\eta)J^+_{00} + \frac{8}{3}\sqrt{2\eta}J^+_{+0} + \frac{2}{3}(2\eta-1)J^+_{+-}\right], \\
G_M &= \frac{1}{2p^+(2\eta+1)}\left[2J^+_{00} + \frac{2(2\eta-1)}{\sqrt{2\eta}}J^+_{+0} - 2J^+_{+-}\right], \\
G_Q &= \frac{1}{2p^+(2\eta+1)}\left[-J^+_{00} + \sqrt{\frac{2}{\eta}}J^+_{+0} - \frac{\eta+1}{\eta}J^+_{+-}\right],
\end{aligned} \tag{2.4}$$

where j^{μ} is the e.m. current, $|p\ \lambda >$ stands for the deuteron state with the momentum p and helicity λ, $J^+_{\lambda'\lambda} \equiv J^0_{\lambda'\lambda} + J^3_{\lambda'\lambda}$ and $p^+ \equiv p^0 + p^3$.

3 Asymptotic behavior

Recently, Brodsky and Hiller [10] have mentioned that in the analysis of the high energy elastic *ed*-cross section at least two momentum scales must be distinguished. The first one is given by the QCD scale $\Lambda_{QCD} \approx 200 MeV/c$ and determines the perturbative QCD regime. In particular, according to the arguments of Ref. [7], this scale controls a high Q^2 suppression of the helicity-flip transition amplitudes

$$J^+_{+0} \approx a\left(\frac{\Lambda_{QCD}}{\sqrt{Q^2}}\right)J^+_{00}, \quad J^+_{+-} \approx b\left(\frac{\Lambda_{QCD}}{\sqrt{Q^2}}\right)^2 J^+_{00}, \tag{3.1}$$

where a and b are some constants.

The second scale is purely kinematical and defined by the deuteron mass M. It was argued [10, 11] that in the region

$$Q^2 \gg 2M\Lambda_{QCD} \approx 0.8(GeV/c)^2 \tag{3.2}$$

the helicity-conserving transition amplitude J^+_{00} dominates, so the quark content of the deuteron could reveal itself already in the experimentally accessible region.

From (2.4) and the QCD-motivated relations (3.1) it follows that the charge form factor G_C should have the lowest leading fall-off degree, while the form factors G_M and G_Q are suppressed by a factor $(Q^2)^{-1}$. At the same time at high Q^2 the meson-nucleon

approach (see e.g. Ref. [12]) predicts that $G_C \propto G_M$ and G_Q is suppressed by a factor $(Q^2)^{-1}$. Thus QCD and the classical nuclear physics give the different predictions for high-Q^2 behavior of such quantities as the ratio B/A and T_{20}.

It was assumed [10, 11] that in (2.4) the helicity-flip transition amplitudes J^+_{+0} and J^+_{+-} could be omitted for the kinematical region (3.2). In this case J^+_{00} cancels in the expressions for T_{20} and B/A. However, the calculated behavior of the last one contradicts the experimental data.

In Ref. [13] it was mentioned that the helicity-flip matrix element J^+_{+0} cannot be neglected in the magnetic form factor. Moreover, it was demonstrated that J^+_{+0} matrix element strongly affects the behavior of the magnetic form factor at Q^2 of a few $(GeV/c)^2$ and provides a neat parametrization for B/A ratio. On the one hand, this kinematical region cannot be considered as a region of pure nucleon-meson physics; on the second hand, it cannot be considered as a region of pure perturbative QCD as well. In the next section we shell study the deuteron e.m. form factors in the framework of phenomenological model, which reproduces the results of calculations with realistic NN-potential at low Q^2, and provides the behavior predicted by perturbative QCD at high Q^2.

4 Smooth connection to low-Q^2 region and numerical analysis

Following the idea of the reduced nuclear amplitudes in QCD [14, 15] we define the reduced helicity transition amplitudes g^+_{00}, g^+_{+0} and g^+_{+-}, rewritting (2.4) in the following way

$$\begin{aligned} G_C &= \frac{G^2(Q^2)}{(2\eta+1)}\left[(1-\frac{2}{3}\eta)g^+_{00}+\frac{8}{3}\sqrt{2\eta}g^+_{+0}+\frac{2}{3}(2\eta-1)g^+_{+-}\right], \\ G_M &= \frac{G^2(Q^2)}{(2\eta+1)}\left[2g^+_{00}+\frac{2(2\eta-1)}{\sqrt{2\eta}}g^+_{+0}-2g^+_{+-}\right], \\ G_Q &= \frac{G^2(Q^2)}{(2\eta+1)}\left[-g^+_{00}+\sqrt{\frac{2}{\eta}}g^+_{+0}-\frac{\eta+1}{\eta}g^+_{+-}\right], \end{aligned} \tag{4.1}$$

where $G(Q^2)$ – is a dipole form factor $G(Q^2) = \left(1+\frac{Q^2}{\delta^2}\right)^{-2}$, δ – is some parameter of order of the nucleon mass. For G_M and G_Q to be finite at $Q^2 \to 0$, the reduced helicity transition amplitudes should obey: $g^+_{00} \sim O(1)$, $g^+_{+0} \sim O(Q)$, $g^+_{+-} \sim O(Q^2)$, which justifies the following parametrization:

$$\begin{gathered} g^+_{00} = \sum_{i=1}^{n} \frac{a_i}{\alpha_i^2+Q^2}, \\ g^+_{+0} = Q\sum_{i=1}^{n}\frac{b_i}{\beta_i^2+Q^2}, \quad g^+_{+-} = Q^2\sum_{i=1}^{n}\frac{c_i}{\gamma_i^2+Q^2} \end{gathered} \tag{4.2}$$

with $\{a_i, \alpha_i\}$, $\{b_i, \beta_i\}$, $\{c_i, \gamma_i\}$ being fitting parameters. From the quark counting rules [7] it follows that the fall-off behavior of these amplitudes at high Q^2's is

$$g_{00}^{+} \sim Q^{-2}, \qquad g_{+0}^{+} \sim Q^{-3}, \qquad g_{+-}^{+} \sim Q^{-4},$$

which, together with the requirement of correct static normalization (Sec. 2), impose the set of restrictions on $\{a_i\}$, $\{b_i\}$, $\{c_i\}$

$$\begin{aligned}
&\sum_{i=1}^{n} \frac{a_i}{\alpha_i^2} = 1, \\
&\sum_{i=1}^{n} b_i = 0, \quad \sum_{i=1}^{n} \frac{b_i}{\beta_i^2} = \frac{2-\mu_D}{2\sqrt{2}M}, \\
&\sum_{i=1}^{n} c_i = 0, \quad \sum_{i=1}^{n} c_i \gamma_i^2 = 0, \quad \sum_{i=1}^{n} \frac{c_i}{\gamma_i^2} = \frac{1-\mu_D-Q_D}{4M^2}.
\end{aligned} \tag{4.3}$$

The "masses" $\{\alpha_i\}$, $\{\beta_i\}$ and $\{\gamma_i\}$ define a nonperturbative part of reduced amplitudes. In our calculations we used the following sequence for each group of these parameters:

$$\alpha_n^2 = 2M\mu^{(\alpha)}, \quad \alpha_i^2 = \alpha_1^2 + \frac{\alpha_n^2 - \alpha_1^2}{n-1}(i-1), \quad i = 1, \ldots, n \tag{4.4}$$

(similarly, for β_i and γ_i), where $\mu^{(\alpha)}$, $\mu^{(\beta)}$ and $\mu^{(\gamma)}$ have the dimension of energy and, in accordance with (3.2), are to be of order of Λ_{QCD}. Results of numerical calculations (n=4, parameters appear in Table 1) for A, B and T_{20} at $\theta = 0^o$ are shown on Figs.1-3. Experimental data are taken from Refs. [16, 17, 18]. Figs. 4 and 5 display the behavior of G_C and G_Q. Experimental points are from the analysis of Ref. [18] The dashed-dot lines correspond to the asymptotic QCD behavior of the reduced matrix elements:

$$g_{00}^{+(\infty)} \approx \frac{\sum_{i=1}^{n} a_i}{Q^2}, \quad g_{+0}^{+(\infty)} \approx -\frac{\sum_{i=1}^{n} b_i \beta_i^2}{Q^3}, \quad g_{+-}^{+(\infty)} \approx \frac{\sum_{i=1}^{n} c_i \gamma_i^4}{Q^4}. \tag{4.5}$$

The reduced helicity transition amplitudes g_{00}^{+}, g_{+0}^{+} and g_{+-}^{+} appear in Figs. 6-8.

As was mentioned before, at the region (3.2) the ratios J_{00}^{+}/J_{+0}^{+} and J_{+0}^{+}/J_{+-}^{+} should be controlled by the QCD scale parameter Λ_{QCD} only. Figs. 9 and 10 demonstrate that this QCD prediction works well for J_{+0}^{+}/J_{+-}^{+}, while for the ratio J_{00}^{+}/J_{+0}^{+} the QCD asymptotics starts at somewhat high Q^2. Estimation of the characteristic energy scale Q_{QCD} at which one may expect the asymptotic behavior of the observables of the elastic *ed*-scattering may be determined from

$$\max\left(\frac{\int_{Q_{QCD}}^{\infty} \left| g_{00}^{+(\infty)} - g_{00}^{+} \right| \, dQ}{\int_{Q_{QCD}}^{\infty} \left| g_{00}^{+} \right| \, dQ}, \; \frac{\int_{Q_{QCD}}^{\infty} \left| g_{+0}^{+(\infty)} - g_{+0}^{+} \right| \, dQ}{\int_{Q_{QCD}}^{\infty} \left| g_{+0}^{+} \right| \, dQ}, \right.$$

$$\left. \frac{\int_{Q_{QCD}}^{\infty} \left| g_{+-}^{+(\infty)} - g_{+-}^{+} \right| \, dQ}{\int_{Q_{QCD}}^{\infty} \left| g_{+-}^{+} \right| \, dQ} \right) \leq \varepsilon,$$

where ε stands for experimental data accuracy. Using the best-fit parameters (see Table 1) and taking different values of ε we made estimations (see. Table 2) of Q_{QCD}, based on all experimental data available.

Table 1

$\backslash i$	1	2	3	4
$a_i\ fm^{-2}$	2.4818	-10.850	6.4416	see (4.3)
$b_i\ fm^{-1}$	-1.7654	6.7874	see (4.3)	see (4.3)
c_i	-0.053830	see (4.3)	see (4.3)	see (4.3)
$\alpha_1^2 = 1.8591\ fm^{-2}$			$\mu^{(\alpha)} = 0.58327\ GeV/c$	
$\beta_1^2 = 19.586\ fm^{-2}$			$\mu^{(\beta)} = 0.1\ GeV/c$	
$\gamma_1^2 = 1.0203\ fm^{-2}$			$\mu^{(\gamma)} = 0.17338\ GeV/c$	
$\delta = 0.89852\ GeV/c$				

Table 2

ε	Q_{QCD}
10%	2.92 GeV/c
7%	3.44 GeV/c
5%	4.04 GeV/c
2%	6.28 GeV/c
1%	8.84 GeV/c

Conclusions

In the present paper we have studied the possible description of the existing experimental data of the elastic *ed*-scattering based on the idea of reduced transition amplitudes, the behavior of which at high Q^2 is fixed by the quark counting rules. At low Q^2 our parametrization reproduces the results of the standard nucleon-meson picture.

The above analysis shows that QCD could strongly affect the behavior of the deuteron e.m. form factors when Q^2 is of order of $10(GeV/c)^2$. This value of the transferred momentum scale is mainly defined by the fact that the QCD asymptotics of the helicity non-flip transition amplitude J^+_{00} starts rather late. Therefore, at intermediate energy the observables independent of J^+_{00} should be sufficiently sensitive to the quark structure of the deuteron. The existing experimental data for the ratio J^+_{+0}/J^+_{+-} are close to the asymptotic prediction (3.1) at $Q^2 \approx 1(GeV/c)^2$. Nevertheless, all experimental points are also in satisfactory correspondence with conventional NN-potential models. The essential discrepancy between what is predicted from QCD and and/or nucleon-meson picture starts at $Q^2 \approx 4(GeV/c)^2$. QCD predicts that from $Q^2 \approx 2(GeV/c)^2$ the ratio J^+_{+0}/J^+_{+-} will tend monotonically to its asymptotic behavior $(J^+_{+0}/J^+_{+-})_{asymp} = 4.51 \times 10^{-2}(Q/\Lambda_{QCD})$. From the other hand, from the NN-potential models it follows that from $Q^2 \approx 4(GeV/c)^2$ this should be an oscillating function.

Acknowledgments

The authors express their thank to C. Carlson and F. Gross for useful discussions.

Figure captions

Figure 1. Structure function $A(Q^2)$ of the elastic *ed*-scattering in the approach of the reduced transition amplitudes (solid line). The dashed line corresponds to the calculations with Paris potential.

Figure 2. Structure function $B(Q^2)$. (For notations see the caption of Fig.1).

Figure 3. Tensor analyzing power T_{20}. (For notations see the caption of Fig.1).

Figure 4. Charge form factor of the deuteron G_C in the approach of the reduced transition amplitudes (solid line). The dashed-dot line stand for QCD asymptotics (see the text for explanation).

Figure 5. Quadrupole form factor of the deuteron G_Q. (For notations see the caption of Fig.4).

Figure 6. The g^+_{00} reduced transition amplitude (solid line). The dashed-dot line stands for its pure asymptotical residue (4.11).

Figure 7. The g^+_{+0} reduced transition amplitude. (For notations see the caption of Fig.6).

Figure 8. The g^+_{+-} reduced transition amplitude. (For notations see the caption of Fig.6).

Figure 9. The ratio of helicity transition amplitudes J^+_{00} and J^+_{+0} calculated within the current approximation (solid line). The dashed-dot line corresponds to the asymptotics (4.11). (The full circles are to distinguish the negative values of the experimental data).

Figure 10. The ratio of the helicity-flip transition amplitudes J^+_{+0} and J^+_{+-} corresponding to the current approach (solid line) and to the approach with Paris potential (dashed line). The dashed-dot line stands for the asymptotics (4.11).

References

[1] A. P. Kobushkin, *Yad. Fiz.* **28**, 495 (1978) [*Sov. J. Nucl. Phys.* **28**, 252 (1978)]. A. P. Kobushkin and V. P. Shelest, *Fiz. Elem. Chastits At. Yadra*, **14**, 1146 (1983) [*Sov. J. Part. Nucl.* **14**, 483 (1983)].

[2] Y. Kizukuri, M. Namiki and K. Okano, *Prog. Theor Phys.*, **61**, 559 (1979).

[3] V. V. Burov, S. M. Dorkin and V. N. Dastasvalov, *Z. Phys.* A - Atoms and Nuclei, **315**, 205 (1984).

[4] A. P. Kobushkin, in *Proceedings of the International Workshop DEUTERON'91*, Dubna, Russia, 1991.

[5] B. A. Matveev, R. M. Muradjan and A. N. Tavkhelidze, *Lett. Nuov. Cim.* **7**, 719 (1973); S. J. Brodsky and G. R. Farrar, *Phys. Rev. Lett.* **31**, 1153 (1973).

[6] A. I. Vainshtein and V. I. Zakharov, *Phys. Lett.* **72B**, 368 (1978).

[7] C. E. Carlson and F. Gross, *Phys. Rev. Lett.* **53**, 127 (1984).

[8] R. Woloshin, *Phys. Rev. Lett.* **36**, 220 (1976).

[9] S. D. Drell and T. M. Yan, *Phys. Rev. Lett.* **24**, 181 (1970).

[10] S. J. Brodsky and J. R. Hiller, *Phys. Rev.* **D46**, 2141 (1992).

[11] F. Coester, in *Proceedings of the International Conference on Medium and High-Energy Nuclear Physics*, Taipei, Taiwan, 1988, edited by W.-Y.P. Hwang, K.F. Liu and Y. Tseng (World Scientific, Singapore, 1989).

[12] M. Gari and H. Hyuga, *Nucl. Phys.* **A264**, 409 (1976).

[13] A. P. Kobushkin and A. I. Syamtomov, *Phys. Rev.* **D49**, 1637 (1994).

[14] S. J. Brodsky and B. T. Chertok, *Phys. Rev. Lett.* **37**, 269 (1976); *Phys. Rev.* **D14**, 3003 (1976).

[15] S. J. Brodsky and J. Hiller, *Phys. Rev.* **C28**, 475 (1983).

[16] R. G. Arnold *et al.*, *Phys. Rev. Lett.* **58**, 1723 (1987); P. E. Bosted *et al.*, *Phys. Rev.* **C42** 38 (1990); R. Cramer *et al.*, *Z. Phys.* **C29** 513 (1985); S. Platchkov *et al.*, *Nucl. Phys.* **A510**, 740 (1990).

[17] I. The *et al.*, *Phys. Rev. Lett.* **67**, 173 (1991); R. Gilman *et al., ibid.***65**, 1733 (1990); B.B. Voitsekhovshii *et al.*,Pis'ma Zh. Eksp. Teor. Fiz. **43**, 567 (1986) [JETP Lett. **43**, 733 (1986)]; M.E. Schulze *et al.*, *Phys. Rev. Lett.* **52**, 597 (1984).

[18] M. Garçon *et al.*, *Phys. Rev.* **C49**, 2516 (1994).

This figure "fig1-1.png" is available in "png" format from:

http://arXiv.org/ps/hep-ph/9409411v1

This figure "fig2-1.png" is available in "png" format from:

http://arXiv.org/ps/hep-ph/9409411v1

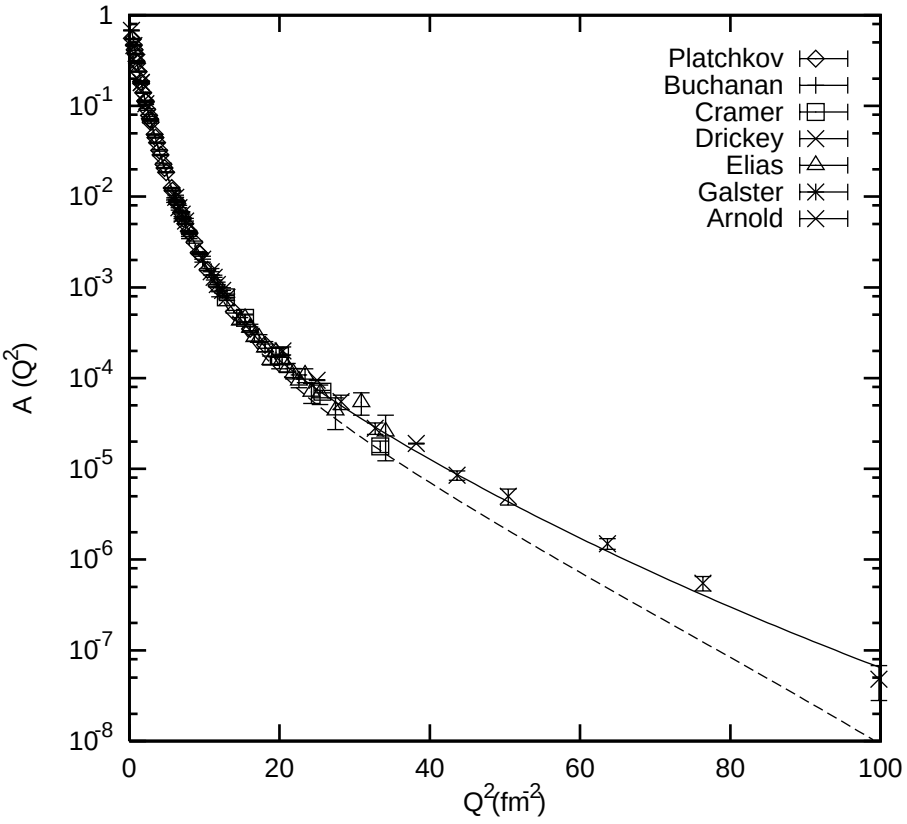
Platchkov
Buchanan
Cramer
Drickey
Elias
Galster
Arnold
A (Q2)
Q2(fm-2)
1
10-1
10-2
10-3
10-4
10-5
10-6
10-7
10-8
0
20
40
60
80
100

Fig. 1

This figure "fig1-2.png" is available in "png" format from:

http://arXiv.org/ps/hep-ph/9409411v1

This figure "fig2-2.png" is available in "png" format from:

http://arXiv.org/ps/hep-ph/9409411v1

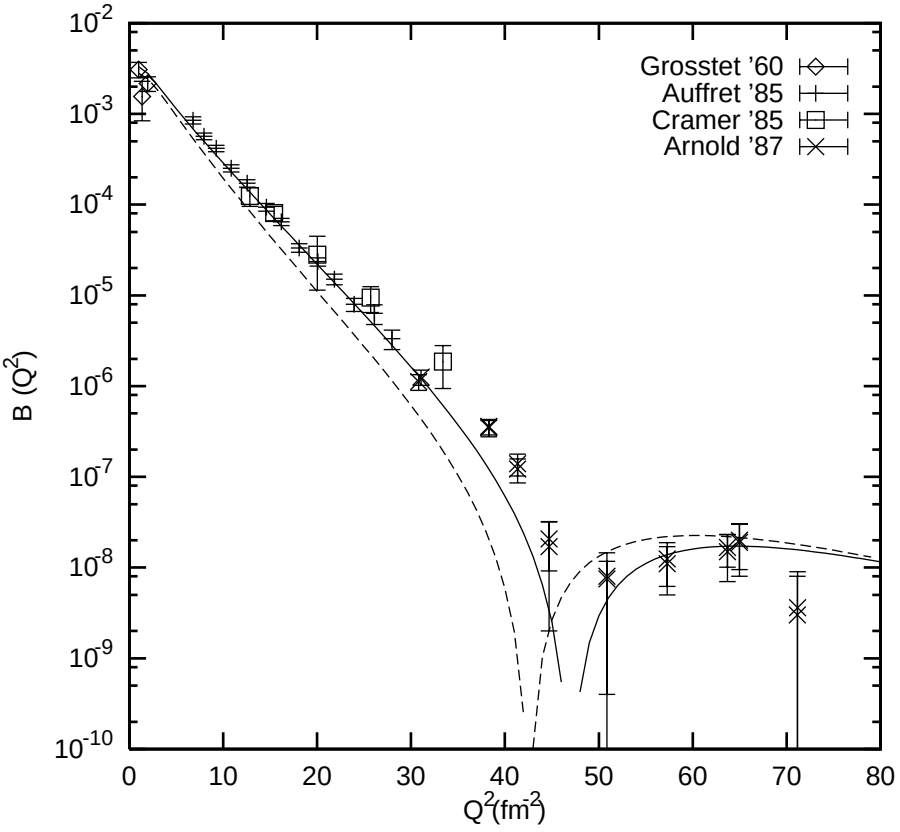
Grosstet '60
Auffret '85
Cramer '85
Arnold '87
B (Q²)
Q²(fm⁻²)
10⁻²
10⁻³
10⁻⁴
10⁻⁵
10⁻⁶
10⁻⁷
10⁻⁸
10⁻⁹
10⁻¹⁰
0
10
20
30
40
50
60
70
80

Fig. 2

This figure "fig1-3.png" is available in "png" format from:

http://arXiv.org/ps/hep-ph/9409411v1

This figure "fig2-3.png" is available in "png" format from:

http://arXiv.org/ps/hep-ph/9409411v1

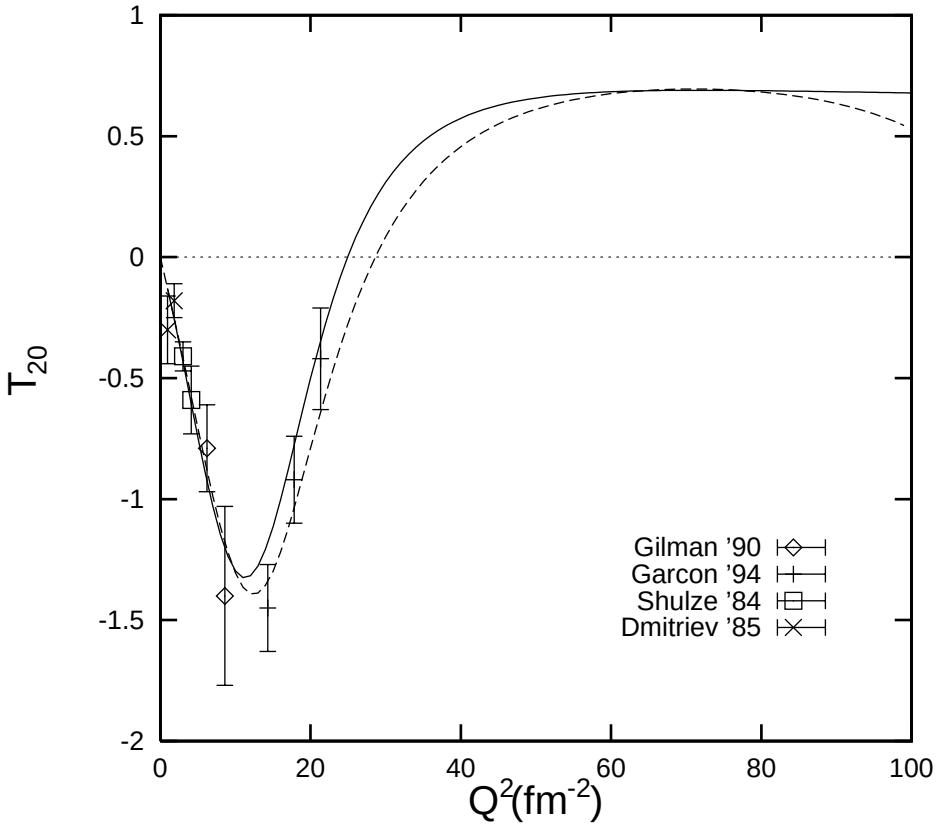
1
0.5
0
-0.5
-1
-1.5
-2
0
20
40
60
80
100
T_{20}
$Q^2(fm^{-2})$
Gilman '90
Garcon '94
Shulze '84
Dmitriev '85

Fig. 3

This figure "fig1-4.png" is available in "png" format from:

http://arXiv.org/ps/hep-ph/9409411v1

This figure "fig2-4.png" is available in "png" format from:

http://arXiv.org/ps/hep-ph/9409411v1

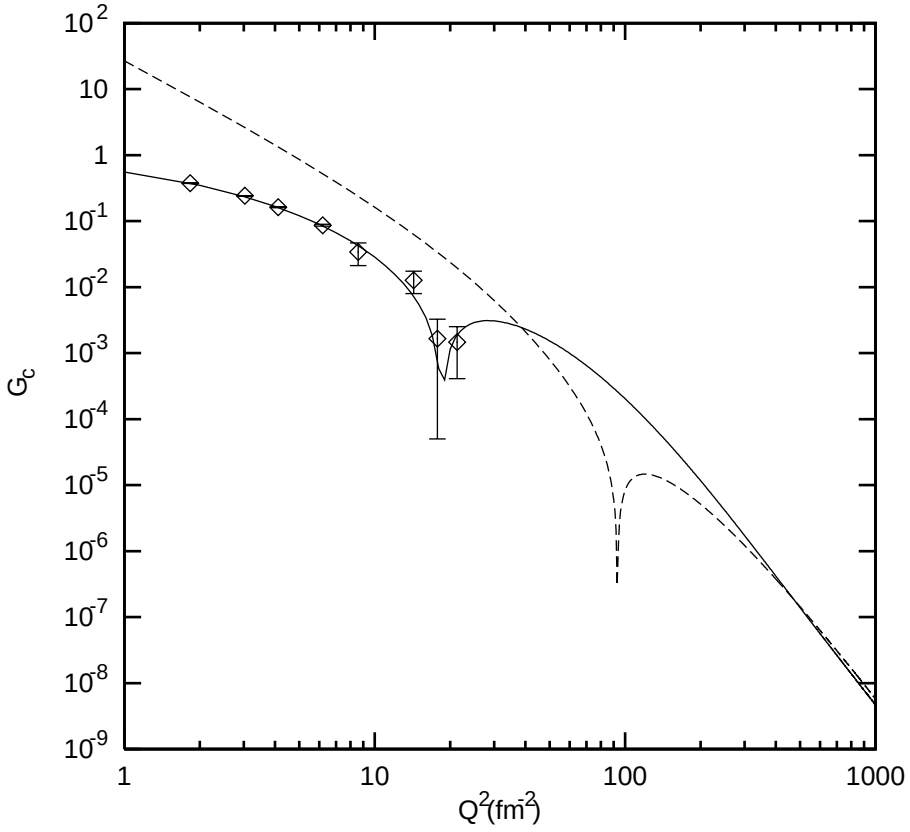
10^2
10
1
10^{-1}
10^{-2}
10^{-3}
10^{-4}
10^{-5}
10^{-6}
10^{-7}
10^{-8}
10^{-9}
G_c
1
10
100
1000
$Q^2(fm^{-2})$

Fig. 4

This figure "fig1-5.png" is available in "png" format from:

http://arXiv.org/ps/hep-ph/9409411v1

This figure "fig2-5.png" is available in "png" format from:

http://arXiv.org/ps/hep-ph/9409411v1

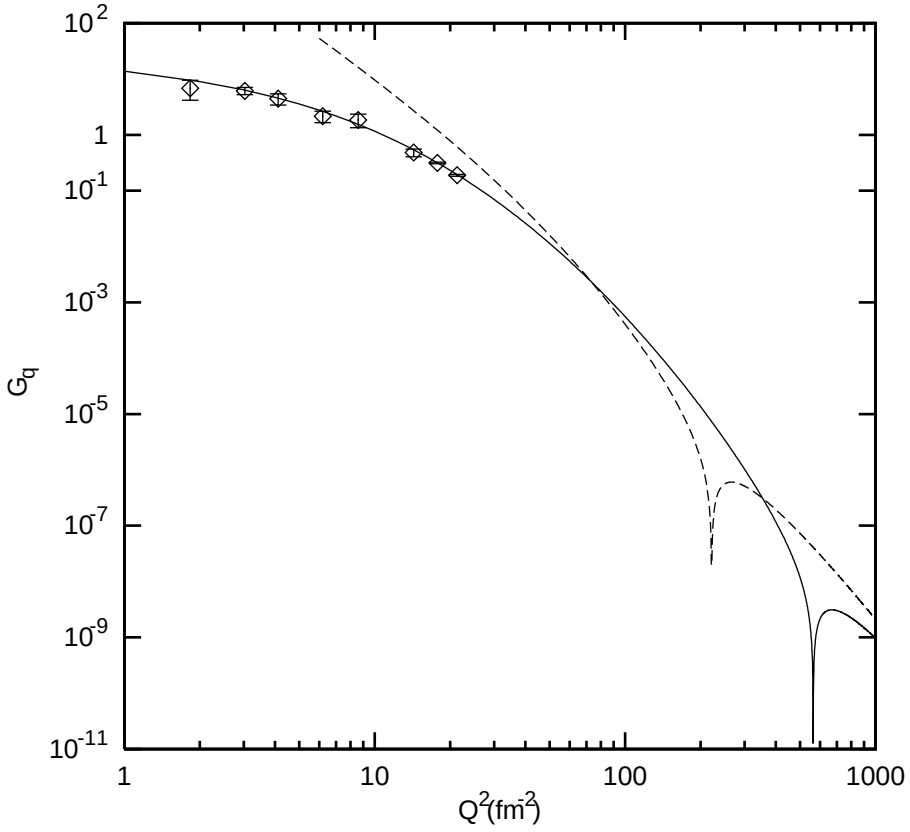

Fig. 5

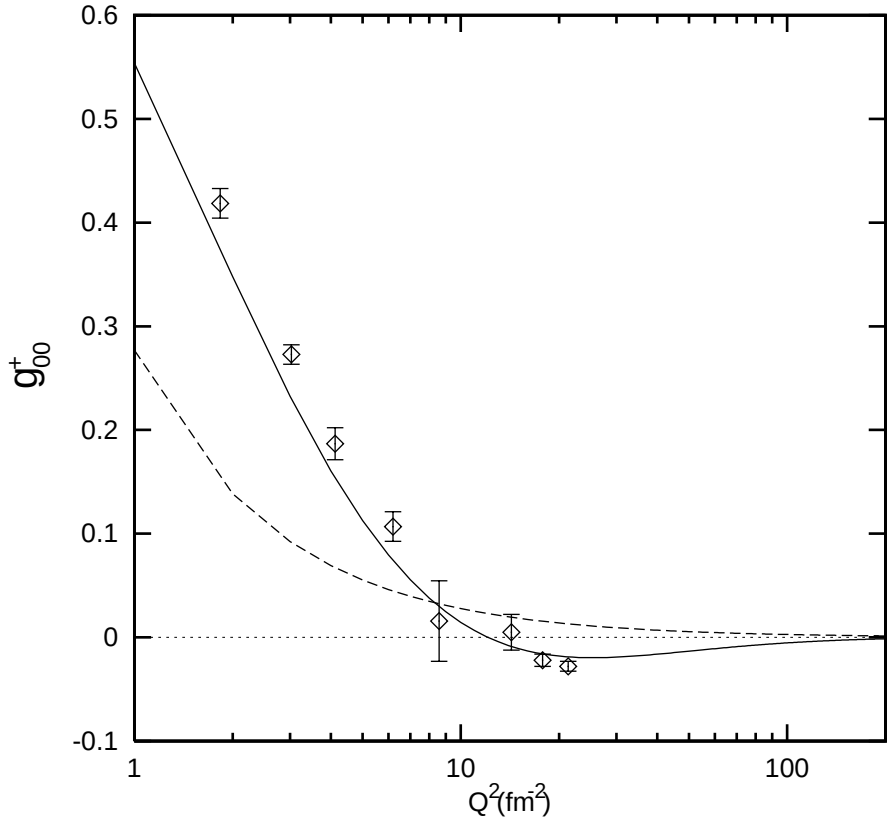

Fig. 6

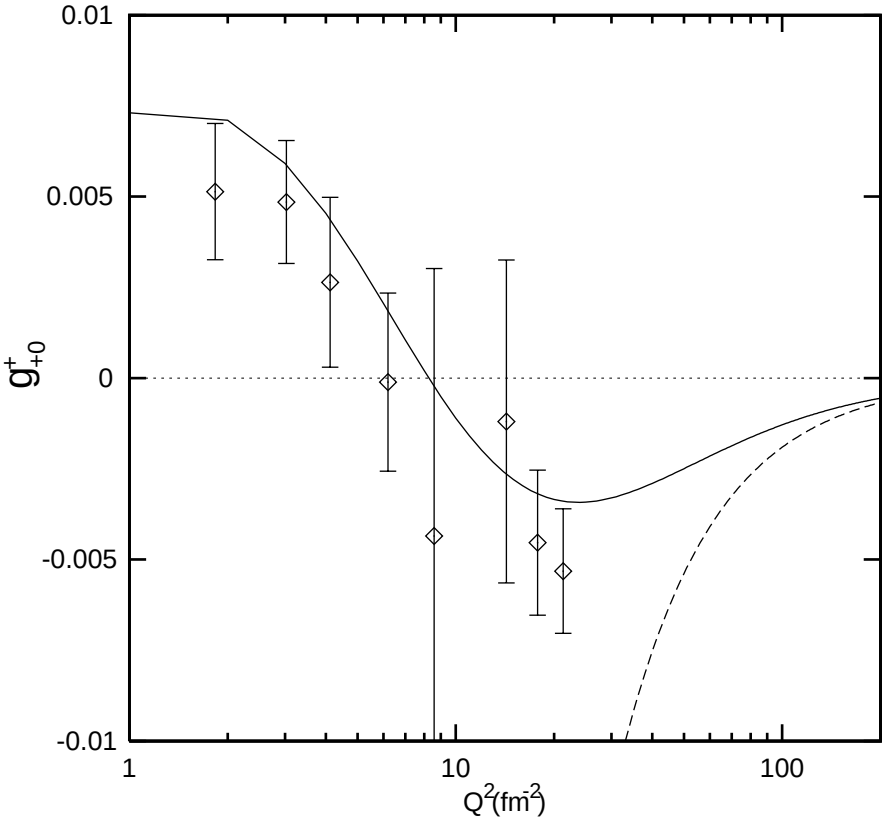

Fig. 7

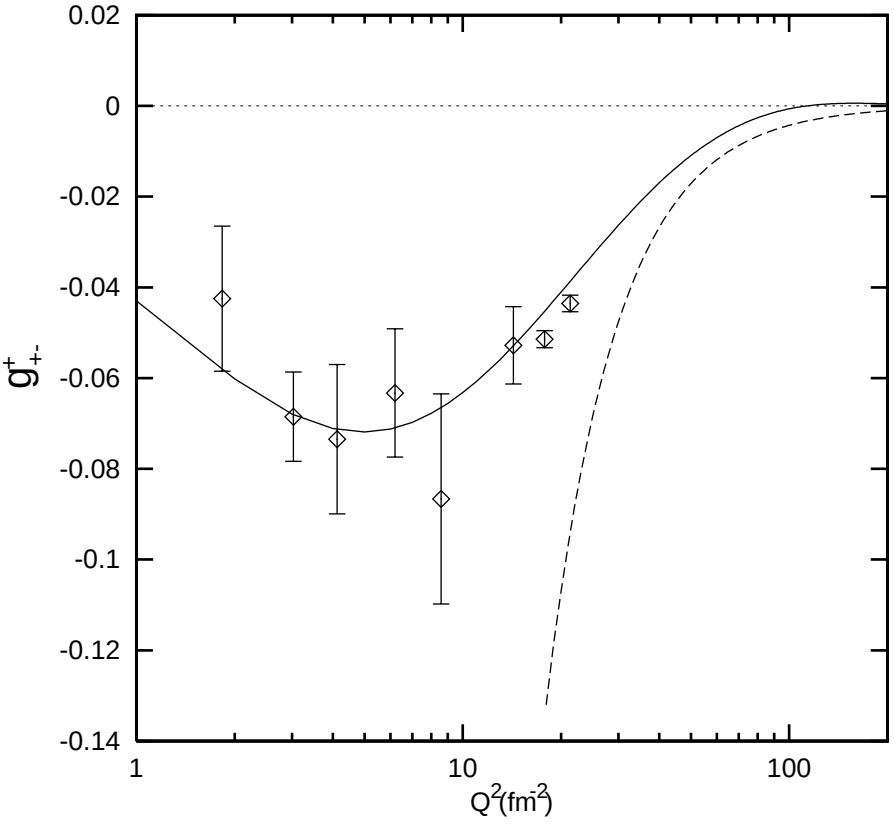

Fig. 8

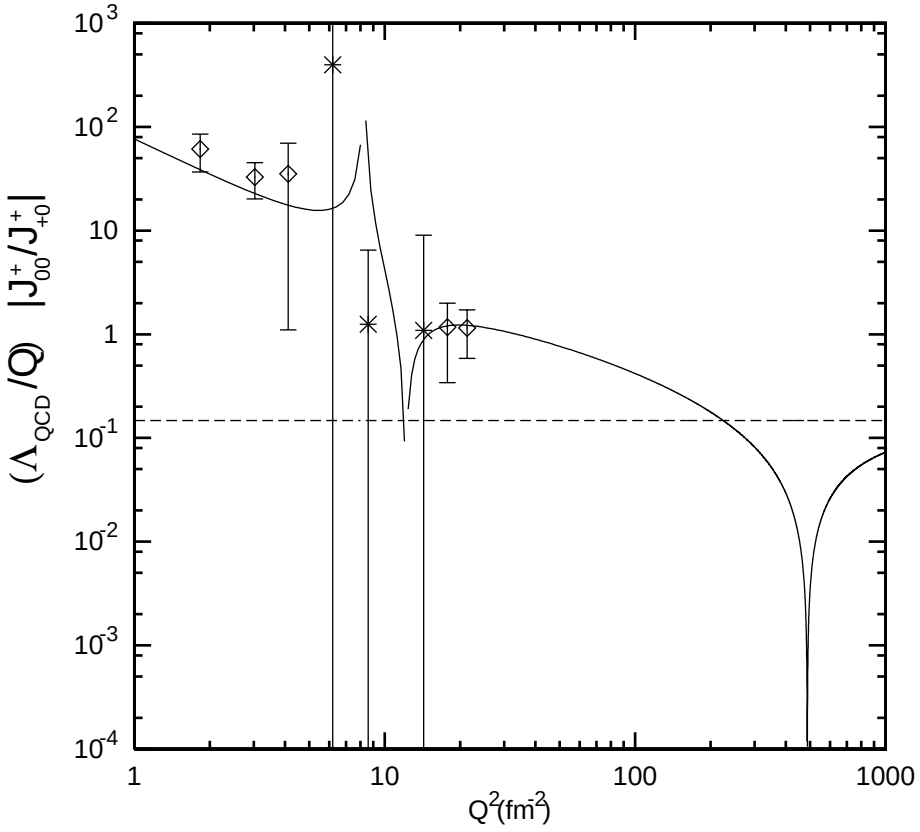
10^3
10^2
10
1
10^{-1}
10^{-2}
10^{-3}
10^{-4}
1
10
100
1000
$Q^2(fm^{-2})$
$(\Lambda_{QCD}/Q)^2 |J^+_{00}/J^+_{+0}|$

Fig. 9

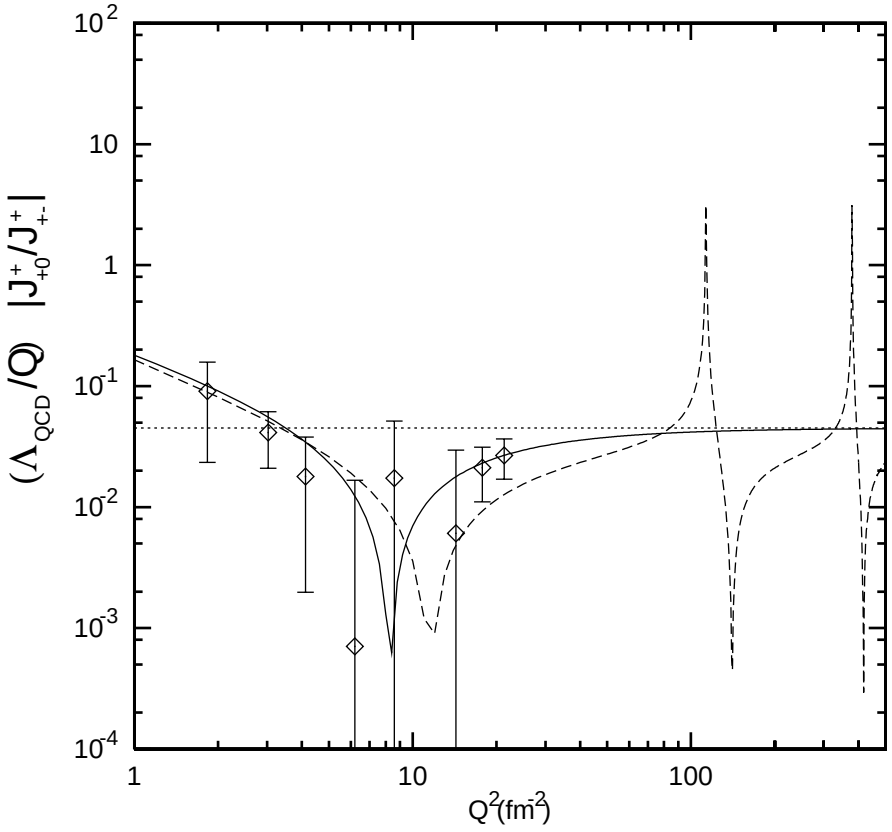

Fig. 10